

Metal–heptaiodide interactions in cyclomaltoheptaose (β -cyclodextrin) polyiodide complexes as detected via Raman spectroscopy

Vasileios G. Charalampopoulos,^a John C. Papaioannou,^{a,*} Glikeria Kakali^b and Haido S. Karayianni^c

^aLaboratory of Physical Chemistry, Department of Chemistry, National and Kapodistrian University of Athens, PO Box 64004, 157 10 Zografou, Athens, Greece

^bLaboratory of Inorganic and Analytical Chemistry, School of Chemical Engineering, National Technical University of Athens, Iroon Polytechniou 9, Zografou 157 80, Athens, Greece

^cLaboratory of Physical Chemistry, School of Chemical Engineering, National Technical University of Athens, Iroon Polytechniou 9, Zografou 157 80, Athens, Greece

Received 22 October 2007; accepted 12 November 2007

Available online 21 November 2007

Abstract—The Raman spectra of the cyclomaltoheptaose (β -cyclodextrin, β -CD) polyiodide complexes (β -CD)₂·NaI₇·12H₂O, (β -CD)₂·RbI₇·18H₂O, (β -CD)₂·SrI₇·17H₂O, (β -CD)₂·BiI₇·17H₂O and (β -CD)₂·VI₇·14H₂O (named β -M, M stands for the corresponding metal) are investigated in the temperature range of 30–140 °C. At room temperature all systems show an initial strong band at 178 cm⁻¹ that reveals similar intramolecular distances of the disordered I₂ units (~2.72 Å). During the heating process β -Na and β -Rb display a gradual shift of this band to the final single frequency of 166 cm⁻¹. In the case of β -Sr and β -Bi, the band at 178 cm⁻¹ is shifted to the final single frequencies of 170 and 172 cm⁻¹, respectively. These band shifts imply a disorder–order transition of the I₂ units whose I–I distance becomes elongated via a symmetric charge-transfer interaction I₂←I₃⁻→I₂. The different final frequencies correspond to different bond lengthening of the disordered I₂ units during their transformation into well-ordered ones. In the Raman spectra of β -V, the initial band at 178 cm⁻¹ is not shifted to a single band but to a double one of frequencies 173 and 165 cm⁻¹, indicating a disorder–order transition of the I₂ molecules via a non-symmetric charge-transfer interaction I₂←I₃⁻→I₂. The above spectral data show that the ability of I₃⁻ to donate electron density to the attached I₂ units is determined by the relative position of the different metal ions and their ionic potential q/r . The combination of the present results with those obtained from our previous investigations reveals that cations with an ionic potential that is lower than ~1.50 (Cs⁺, Rb⁺, Na⁺, K⁺ and Ba²⁺) do not affect the Lewis base character of I₃⁻. However, when the ionic potential of the cation is greater than ~1.50 (Li⁺, Sr²⁺, Cd²⁺, Bi³⁺ and V³⁺), the Mⁿ⁺··I₃⁻ interactions become significant. In the case of a face-on position of the metal (Sr²⁺, Bi³⁺) relative to I₃⁻, the charge-transfer interaction is symmetric. On the contrary, when the metal (Li⁺, Cd²⁺, V³⁺) presents a side-on position relative to I₃⁻, the charge-transfer interaction is non-symmetric.

© 2007 Elsevier Ltd. All rights reserved.

Keywords: Cyclomaltooligosaccharides; β -Cyclodextrins; Heptaiodide ions; Raman spectroscopy; Inclusion complexes; Disorder–order

1. Introduction

The polyiodide inclusion complexes of cyclomaltoheptaose (β -cyclodextrin, β -CD) with various metal ions

display isomorphous crystal structures (monoclinic $P2_1$) that consist of non-interacting heptaiodide units of Z-shape.^{1–4} In these channel-type systems, the β -CD molecules are arranged head to head, producing dimers that are stacked like coins in a roll and form slightly zigzagged cylinders.¹ The I₇⁻ ions can be formulated as I₂·I₃⁻·I₂ with the I₂ and I₃⁻ nearly perpendicular to each

* Corresponding author. Tel.: +30 210 7274561; fax: +30 210 7274752; e-mail: jpapaioannou@chem.uoa.gr

other (Fig. 1). More explicitly, the central I_3^- unit is well-ordered and located in the space between two neighbouring β -CD dimers (near their O(6) rims). The two disordered I_2 units are attached to the I_3^- ion and included within the cavities of the dimers (near their O(2), O(3) rims). The counterions are located between the dimers but outside the β -CD cylinders interacting with the O(6)H hydroxyl groups and the water molecules of the interstices.

In our previous papers, we have investigated a variety of β -cyclodextrin polyiodide complexes with different metal ions (Ba^{2+} , Cd^{2+} , K^+ , Li^+ and Cs^+)^{2–4} by using several techniques to achieve a thorough characteriza-

tion of their physicochemical properties. Raman spectroscopy has proven to be one of the most powerful methods for the detection of the heptaiodide structural changes with temperature. Our spectroscopic study has been focused on the frequency range of 140–210 cm^{-1} , where the perturbations of the iodine molecules can be observed. The β -CD molecules exhibit significantly intense bands in a range of higher frequencies (2800–3500 cm^{-1}) according to the detailed investigation of Moreira da Silva et al.⁵ At room temperature, all of these systems showed a strong band at 178–179 cm^{-1} that was assigned to the ν_1 mode of the disordered iodine molecules in the heptaiodides. This frequency

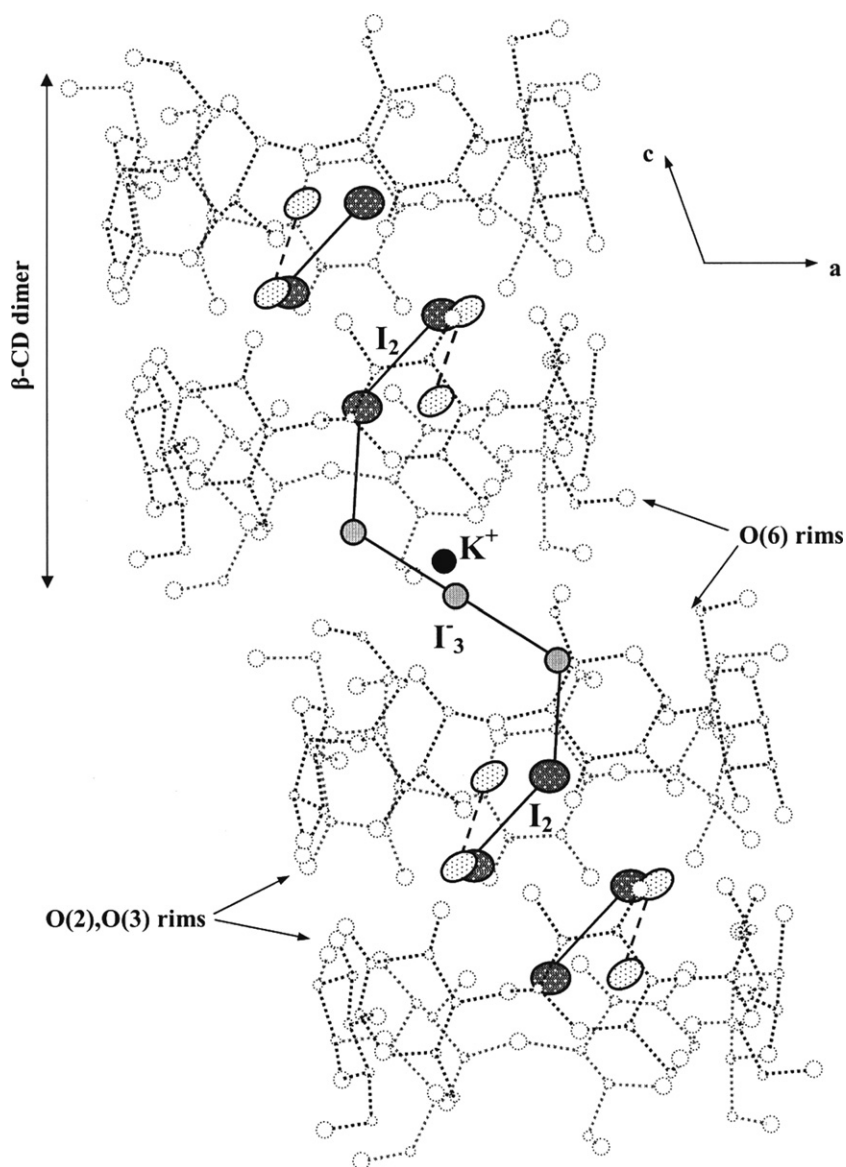


Figure 1. The geometry of the heptaiodide ions (along the b -axis) embedded in the β -CD dimers of the monoclinic $(\beta\text{-CD})_2\text{KI}_7\cdot 9\text{H}_2\text{O}$, according to the single-crystal X-ray analysis.¹ The white ellipsoids with the black spots correspond to the disordered iodine atoms of I_2 that are in positions of minor occupancies ($d(I-I) < 2.77 \text{ \AA}$). The grey ellipsoids with the white spots correspond to the disordered iodine atoms of I_2 that are in positions of main occupancies ($d(I-I) = 2.77 \text{ \AA}$). The well-ordered atoms of I_3^- are presented as grey spheres, whereas the potassium ion is presented as a black sphere.

slightly deviates from the value of 180 cm^{-1} , which is the characteristic spectral feature of the diiodine in the solid state,⁶ as a result of the different local environments in each system (e.g., $\text{I}_2 \cdots \text{I}_3^-$ in the β -CD hepta-iodide complexes and $\text{I}_2 \cdots \text{I}_2$ in solid diiodine). During the heating process, the complexes with Ba^{2+} , K^+ and Cs^+ displayed a gradual shift of the band at $178\text{--}179\text{ cm}^{-1}$ to the final single frequency of $165\text{--}166\text{ cm}^{-1}$ due to a charge-transfer interaction between the I_3^- ion and the two I_2 units. These spectral data revealed a disorder–order transition of the I_2 units that resulted in an equal lengthening of their bond distances. On the contrary, in the case of

the complexes with Li^+ and Cd^{2+} , the initial band ($178\text{--}179\text{ cm}^{-1}$) was shifted to a double band of frequencies $168, 165\text{ cm}^{-1}$ and $170, 165\text{ cm}^{-1}$, respectively. These results indicated that the two I_2 units of each hepta-iodide presented a different elongation during their disorder–order transformation.

In the present work, we extend our Raman study to five more β -CD complexes with Na^+ , Rb^+ , Sr^{2+} , Bi^{3+} and V^{3+} (named β -Na, β -Rb, β -Sr, β -Bi and β -V in our work) to draw some general conclusions about the influence of the metals on the hepta-iodide donor–acceptor properties. For this reason, we take into consider-

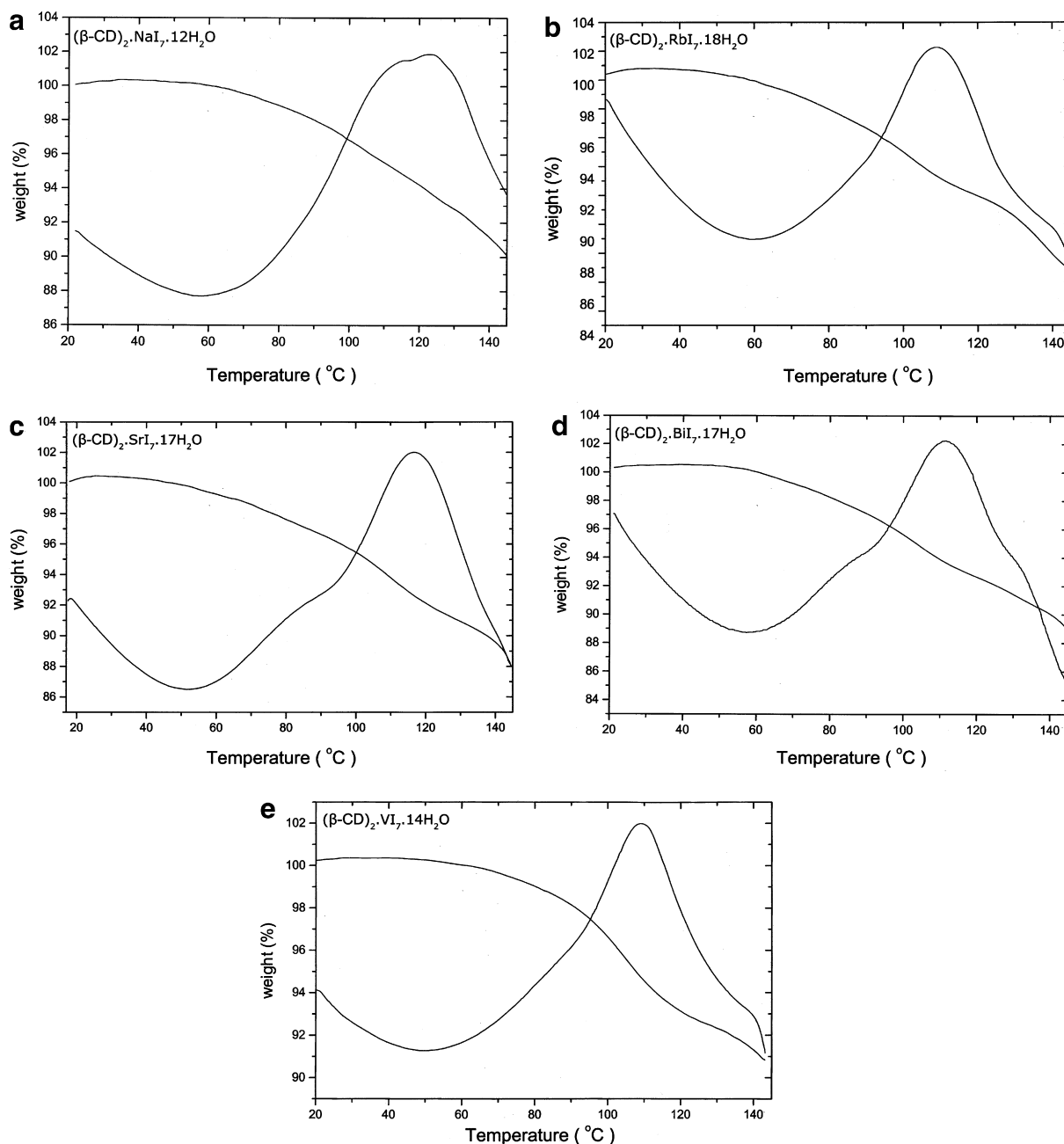


Figure 2. Simultaneous thermogravimetry (TGA) and differential thermal analysis (DTA) of (a) $(\beta\text{-CD})_2\cdot\text{NaI}_7\cdot 12\text{H}_2\text{O}$, (b) $(\beta\text{-CD})_2\cdot\text{RbI}_7\cdot 18\text{H}_2\text{O}$, (c) $(\beta\text{-CD})_2\cdot\text{SrI}_7\cdot 17\text{H}_2\text{O}$, (d) $(\beta\text{-CD})_2\cdot\text{BiI}_7\cdot 17\text{H}_2\text{O}$ and (e) $(\beta\text{-CD})_2\cdot\text{VI}_7\cdot 14\text{H}_2\text{O}$. Heating rate: $5^\circ\text{C}/\text{min}$.

ation the present results combined with those obtained from our previous investigations.

2. Experimental

2.1. Materials and synthesis

β -Cyclodextrin, iodine and sodium iodide (NaI) were purchased from Fluka Chemica, the rubidium and strontium iodides (RbI, SrI₂) were purchased from Alfa Aesar, whereas the bismuth and vanadium iodides (BiI₃, VI₃) were purchased from Aldrich. For the preparation of the β -CD complex with Na⁺ (β -Na), 1 g of β -CD was dissolved in 80 mL of distilled water at room temperature under stirring, until the solution became almost saturated. Then 0.34 g of sodium iodide and 0.44 g of solid iodine were added simultaneously to the solution, and it was heated to 70 °C for 20–25 min. The hot solution was transferred quickly through a folded filter to an empty beaker (100 mL) that was covered with Teflon and then immersed in a Dewar flask (500 mL) containing hot water (~70 °C). After two days very fine reddish-brown thin needles of β -Na were grown, separated in a Buchner filter and dried in air. For β -Rb, β -Sr, β -Bi and β -V the same synthetic route was employed using 1 g of β -CD and 0.44 g of I₂ and 0.48 g of RbI, 0.39 g of SrI₂, 0.45 g of BiI₃ and 0.33 g of VI₃ as appropriate. After two days very fine reddish-brown thin needles of all the above inclusion complexes were grown in a similar way to the β -Na case.

2.2. Characterization methods of the synthesized inclusion complexes

2.2.1. Thermal analysis. Simultaneous thermogravimetry (TGA) and differential thermal analysis (DTA) of the crystals were performed using a NETZSCH-STA 409 EP Controller TASC 414/3 (reference Al₂O₃). The samples (75–100 mg) were heated in the temperature range of 20–145 °C with a heating rate of 5 °C min⁻¹.

2.2.2. X-ray powder diffraction (XRD). A few grams of each one of the five complexes were finely hand-pulverized. The experimental X-ray powder diffraction patterns were obtained at room temperature (25 °C) with a Siemens D 5000 diffractometer using Cu K α 1 radiation ($\lambda = 1.54059 \text{ \AA}$) at 40 kV, 30 mA and a graphite monochromator. The diffraction data were collected in the 2θ range of 5–55° with a constant step of 0.015° and a counting time of 5 s/step.

2.3. Techniques

2.3.1. Raman spectroscopy. The polycrystalline complexes were packed into a high-temperature cell (Venta-

con), and their Raman spectra were obtained at 4 cm⁻¹ resolution from 3500 cm⁻¹ to 100 cm⁻¹ with a data point interval of 1 cm⁻¹ using a Perkin-Elmer NIR FT spectrometer (Spectrum GX II) equipped with an InGaAs detector. The laser power and spot (Nd:YAG at 1064 nm) were controlled to be constant at 50 mW during the measurements, and 400 scans were accumulated. All samples were gradually heated from 30 to 140 °C, by raising the temperature in 10 °C increments in the range of 30–70 °C, in 5 °C increments in the range of 70–110 °C, and in 10 °C increments in the range of 110–140 °C. The temperature variation was controlled

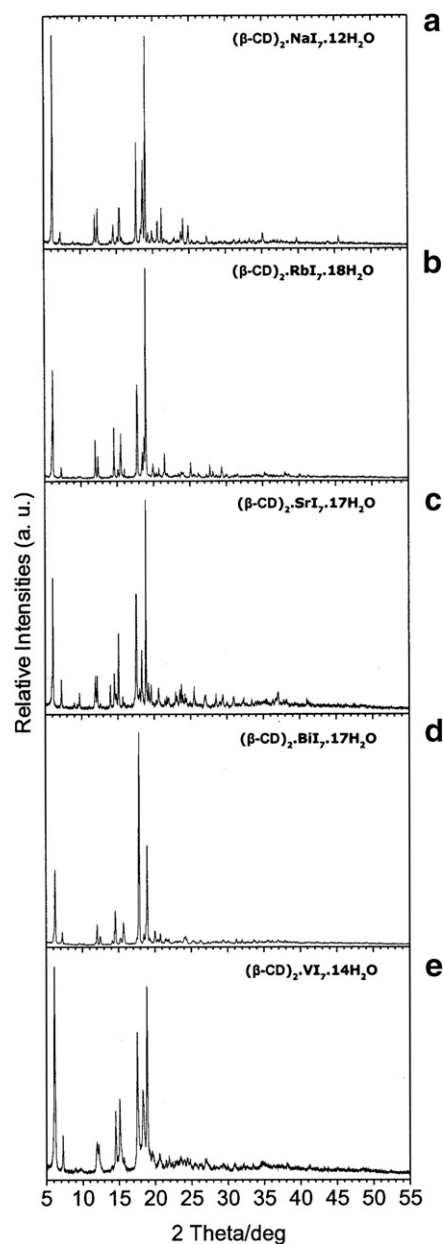


Figure 3. X-ray powder diffraction patterns of (a) (β -CD)₂NaI₇·12H₂O, (b) (β -CD)₂RbI₇·18H₂O, (c) (β -CD)₂SrI₇·17H₂O, (d) (β -CD)₂BiI₇·17H₂O and (e) (β -CD)₂VI₇·14H₂O.

with a Vantacon Winchester instrument equipped with a CALCOMMS 3300 autotune controller.

3. Results

3.1. Thermal analysis

The thermogravimetric analysis (TGA) and differential thermal analysis (DTA) curves of the five β -CD heptaoidide complexes are shown in Figure 2a–e. The evaluation of the number of water molecules per dimer was directly related to the mass loss in the temperature range of $55\text{ }^{\circ}\text{C} \leq \theta \leq 130\text{ }^{\circ}\text{C}$. The results were in agreement with ~ 12 and $\sim 18\text{H}_2\text{O}$ molecules per dimer for β -Na and β -Rb (Fig. 2a and b), respectively, $\sim 17\text{H}_2\text{O}$ molecules per dimer for both β -Sr and β -Bi (Fig. 2c and d) and $\sim 14\text{H}_2\text{O}$ molecules per dimer for β -V (Fig. 2e). We point out that the appearance of double endother-

mic peaks at temperatures lower than $130\text{ }^{\circ}\text{C}$, reveals the coexistence of two kinds of water molecules (tightly bound and easily movable) in the crystal lattice.^{2–4,7,8} The third endothermic peak at temperatures higher than $130\text{ }^{\circ}\text{C}$ corresponds to the sublimation of iodine,^{2–4} which causes the decomposition of the polyiodide chains.

3.2. X-ray powder diffraction (XRD)

The experimental X-ray powder diffraction patterns of β -Na, β -Rb, β -Sr, β -Bi and β -V are shown in Figure 3a–e. It is credibly evident that all of the five β -CD heptaoidide complexes are isomorphous since they present Bragg reflections that are located at the same positions (2θ angles) and correspond to the monoclinic $P2_1$ crystalline form of β -K.^{1–4} The preferred orientation effects (texture) within the powder specimens seem to be exclusively responsible for the observed differences in the rel-

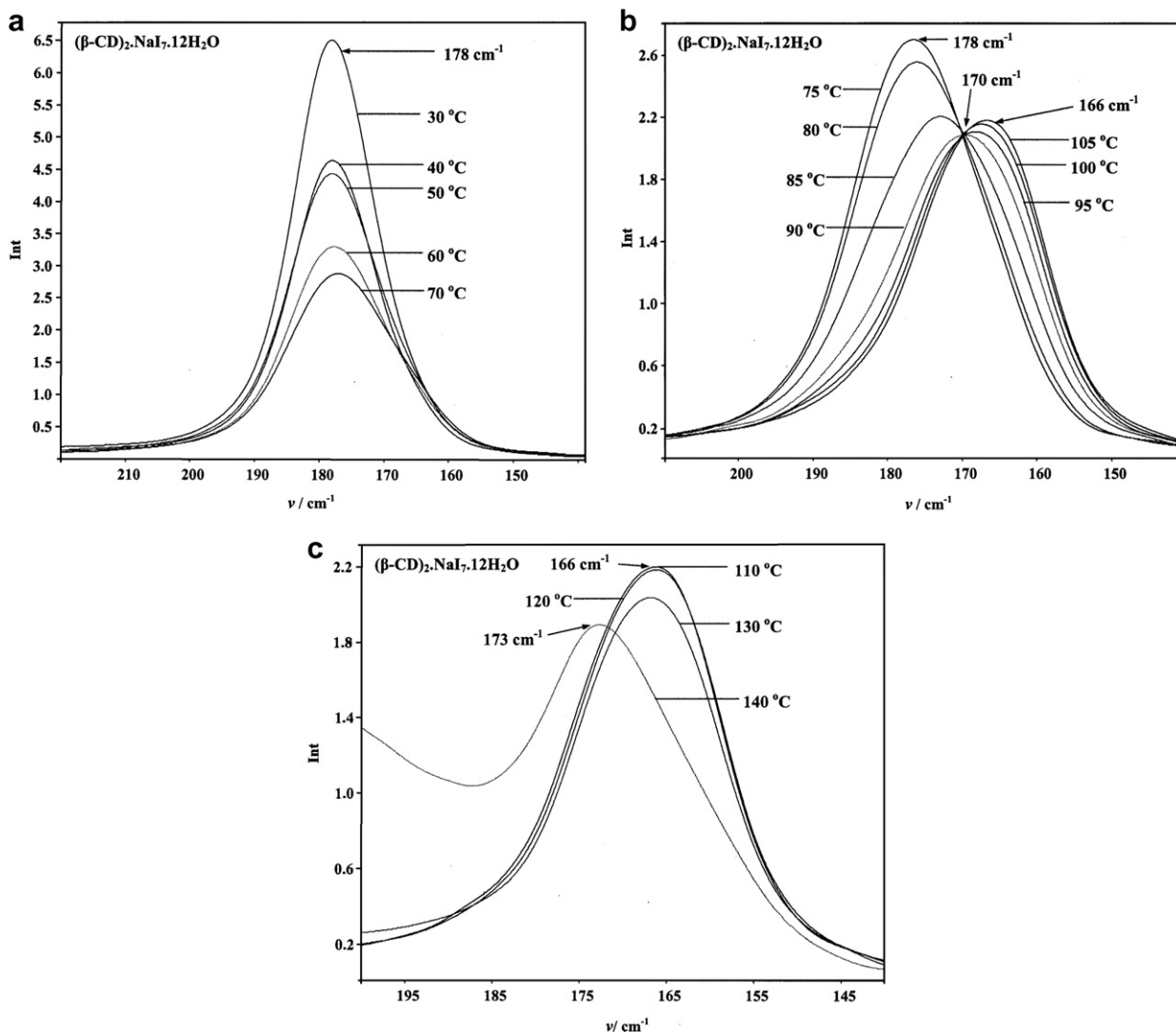


Figure 4. Raman spectra of $(\beta\text{-CD})_2\cdot\text{NaI}_7\cdot 12\text{H}_2\text{O}$ during heating, in the temperature ranges of (a) 30–70 °C, (b) 75–105 °C and (c) 110–140 °C.

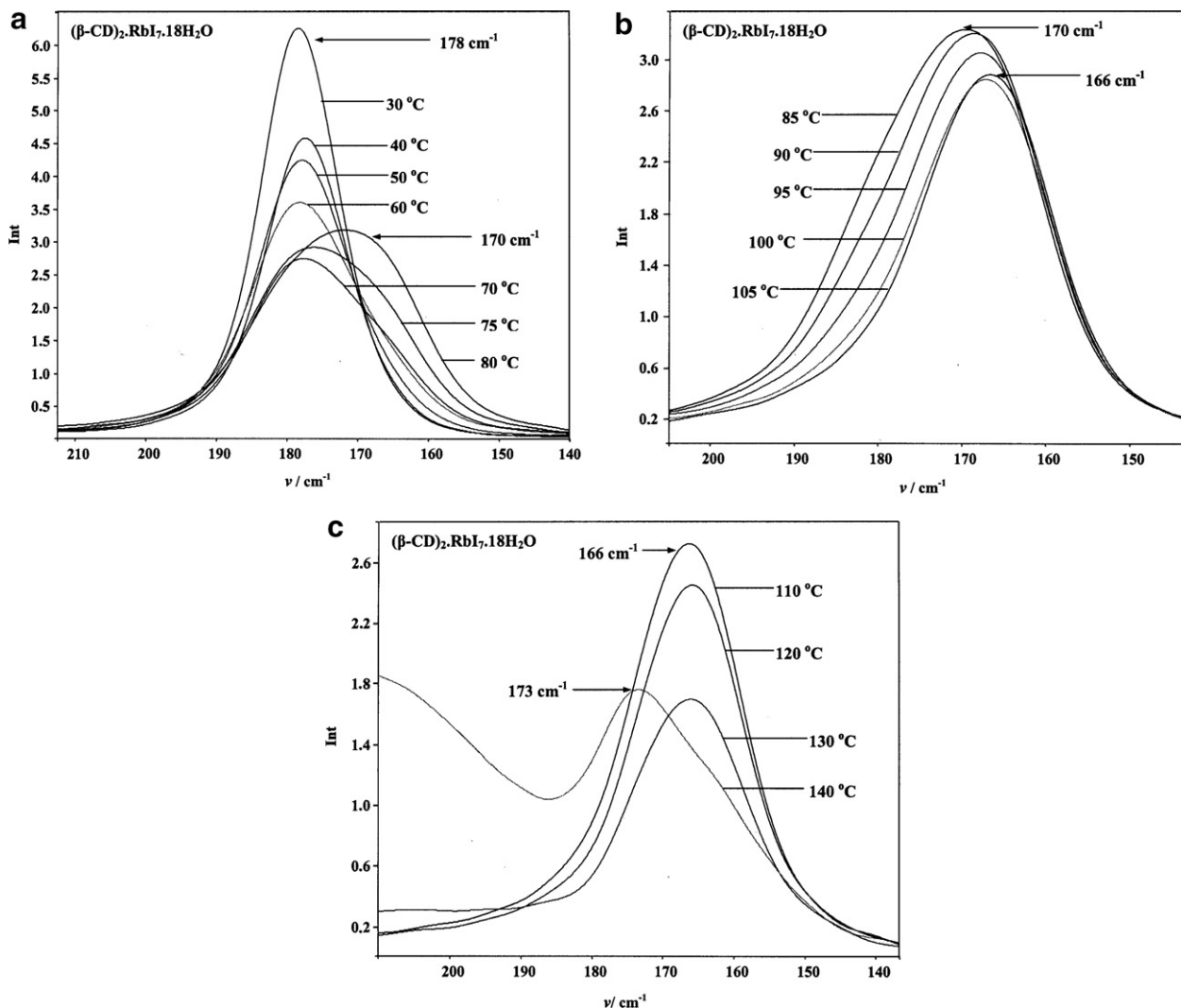


Figure 5. Raman spectra of $(\beta\text{-CD})_2\cdot\text{RbI}_7\cdot 18\text{H}_2\text{O}$ during heating, in the temperature ranges of (a) 30–80 °C, (b) 85–105 °C and (c) 110–140 °C.

ative intensities of some diffraction peaks. However, this is not the only reason for the variation of the intensity data. Thermal analysis showed that each inclusion complex consists of a different number of water molecules per dimer. But despite the fact that the degree of hydration does not affect the crystalline structure,⁹ the water molecules are neither expected to occupy identical positions in the interstices nor to present similar interactions with the metal ions and the $\beta\text{-CD}$ hydroxyl groups. Additionally, Raman spectroscopy reveals that the heptaiodides in the $\beta\text{-CD}$ dimers display structural differences, indicating non-equivalent positions of the iodine atoms. Nevertheless, the isomorphism of these complexes implies that the metal ions are located between the O(6) rims of the neighbouring dimers (but outside the $\beta\text{-CD}$ cylinders), opposite to the I_3^- ions of the I_7^- units.¹ Finally, the total absence of any hump (indicative of amorphous material) proves the purity of the synthesized inclusion complexes (single phases).

3.3. Raman spectroscopy

The Raman spectra of $\beta\text{-Na}$ and $\beta\text{-Rb}$ complexes during the heating process in the range of 30–140 °C are shown in Figures 4a–c and 5a–c, respectively. At 30 °C, $\beta\text{-Na}$ presents a strong band at 178 cm^{-1} with an intensity of 6.50. As the temperature increases to 70 °C, the intensity decreases up to 2.87. In the range of 75–90 °C, the above band is gradually shifted to the frequency of 170 cm^{-1} and the intensity decreases to 2.08. In the range of 95–110 °C, the band is shifted to the final frequency of 166 cm^{-1} and the intensity gradually increases up to 2.19. At 120–130 °C the intensity decreases, whereas at 140 °C the band is shifted to 173 cm^{-1} . In the case of $\beta\text{-Rb}$ there is an initial (30 °C) strong band at 178 cm^{-1} with an intensity of 6.25. In the range of 40–60 °C, the intensity continuously decreases up to 3.60. At 70 °C, a shoulder appears at $\sim 170\text{ cm}^{-1}$ whose intensity increases with temperature, and at 85 °C it

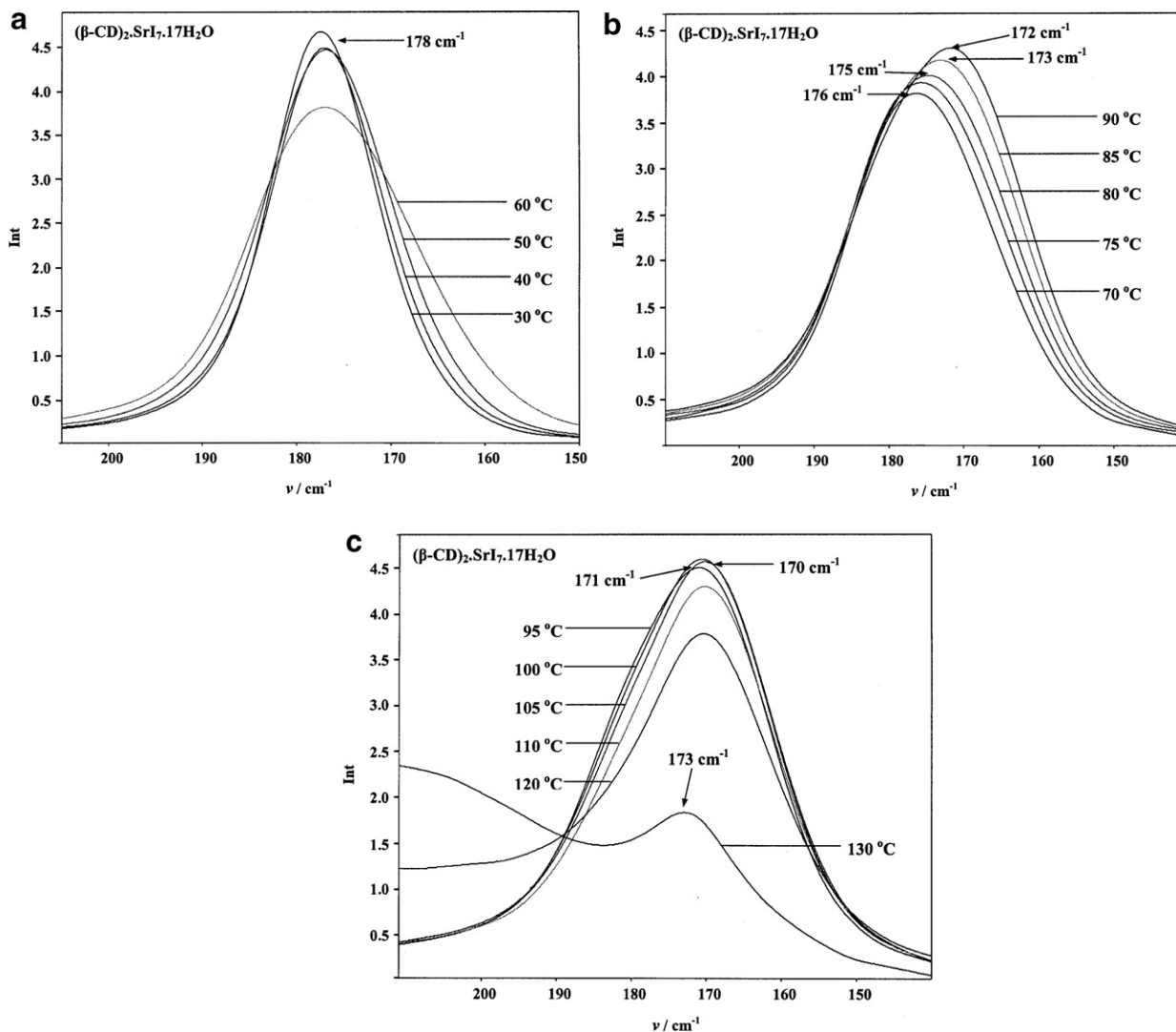


Figure 6. Raman spectra of $(\beta\text{-CD})_2\cdot\text{SrI}_7\cdot 17\text{H}_2\text{O}$ during heating, in the temperature ranges of (a) 30–60 °C, (b) 70–90 °C and (c) 95–130 °C.

becomes the main band. In the range of 90–110 °C, there is a gradual shift to the final frequency of 166 cm^{-1} and a decrease of the intensity to the value of 2.72. At 120–130 °C, the intensity continues to decrease, whereas at 140 °C the band is shifted to 173 cm^{-1} .

The Raman spectra of $\beta\text{-Sr}$ and $\beta\text{-Bi}$ complexes during the heating process in the range of 30–130 °C are shown in Figures 6a–c and 7a–d, respectively. At 30 °C, $\beta\text{-Sr}$ shows a band at 178 cm^{-1} with an intensity of 4.66. As the temperature is raised to 60 °C, the intensity decreases to 3.81. In the range of 70–100 °C, the above band is gradually shifted to the final frequency of 170 cm^{-1} , and the intensity increases to 4.59. At 105–120 °C, the intensity continuously decreases, whereas at 130 °C the band is shifted to 173 cm^{-1} . Concerning $\beta\text{-Bi}$, there is an initial (30 °C) band at 178 cm^{-1} with an intensity of 3.03. In the range of 30–60 °C, the intensity of this band remains almost constant. At temperatures of 70, 80, 85 and 90 °C, this band is gradually

shifted to the frequencies of 177, 176, 175 and 174 cm^{-1} , respectively, with almost constant intensity. At 95 °C, there is a band at 173 cm^{-1} with an intensity of 3.11, whereas in the range of 100–130 °C a band at 172 cm^{-1} is observed whose intensity gradually decreases to the final value of 1.41.

Finally, the Raman spectra of $\beta\text{-V}$ during the heating process in the range of 30–130 °C are shown in Figure 8a–c. At 30 °C, there is a strong band at 178 cm^{-1} with an intensity of 3.01. From 40 to 70 °C, the intensity gradually decreases to the value of 2.14. At 75 °C, a shoulder appears at 165 cm^{-1} (0.92), whereas the initial band (178 cm^{-1}) is shifted to 176 cm^{-1} (1.87). In the range of 80–100 °C, the intensities of the main band and the shoulder continuously decrease, whereas the main band is gradually shifted to the final frequency of 173 cm^{-1} . At 110 °C the intensities of the band at 173 cm^{-1} and the shoulder at 165 cm^{-1} increase (1.58 and 1.09, respectively), whereas at 120–130 °C they decrease again.

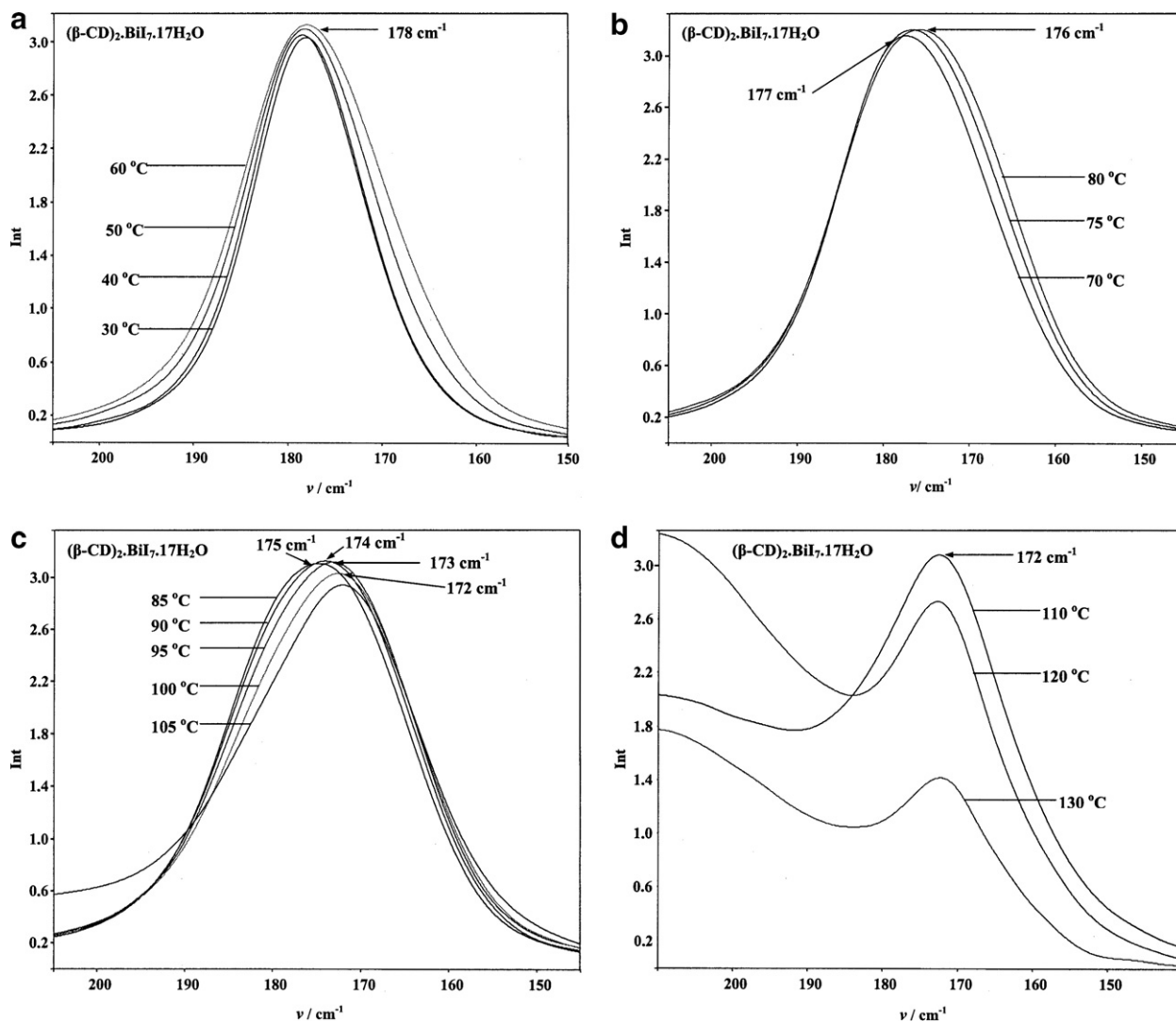


Figure 7. Raman spectra of $(\beta\text{-CD})_2\cdot\text{BiI}_7\cdot 17\text{H}_2\text{O}$ during heating, in the temperature ranges of (a) 30–60 °C, (b) 70–80 °C, (c) 85–105 °C and (d) 110–130 °C.

4. Discussion

4.1. Symmetric $\text{I}_2 \cdots \text{I}_3^-$ interactions

It is already known that as I_2 becomes coordinated to an electron donor (e.g., I_3^-), the intraiodine distance increases and the ν_1 mode moves to lower wavenumbers with respect to the value of 180 cm^{-1} , which is reported for solid diiodine.⁶ The temperature-dependent Raman spectra of $\beta\text{-Na}$ and $\beta\text{-Rb}$ present a gradual shift of the initial band at 178 cm^{-1} to the final value of 166 cm^{-1} . These experimental results are identical to those that have been previously found for the isomorphous $\beta\text{-Ba}$, $\beta\text{-K}$ and $\beta\text{-Cs}$ complexes and the above frequencies have been directly related to the intramolecular distance of the I_2 units.^{2–4} According to the empirical correlation $\nu(\text{I-I}) - d(\text{I-I})$ for weak–medium strength charge-transfer

compounds, suggested by Deplano and co-workers,^{10,11} the frequency of 178 cm^{-1} corresponds to the distance of 2.72 \AA , whereas the frequency of 166 cm^{-1} corresponds to the distance of 2.77 \AA . Additionally, the single-crystal X-ray analysis of the isomorphous $\beta\text{-K}$ has revealed that the disordered iodine atoms of I_2 , which are in positions of main occupancies, present an I–I distance of 2.77 \AA (for minor occupancies the distance is shorter and not estimated).¹ Therefore, we have assigned the band shift $178 \rightarrow 166\text{ cm}^{-1}$ to a disorder–order transition of the I_2 units via a thermally activated charge-transfer interaction ($\text{I}_2 \leftarrow \text{I}_3^- \rightarrow \text{I}_2$). More specifically, their I atoms with minor occupancies are transformed into those with main occupancies as the temperature is raised, implying an elongation of the I–I distance from the initial mean value of 2.72 \AA (disordered state) to the final value of 2.77 \AA (well-ordered state):

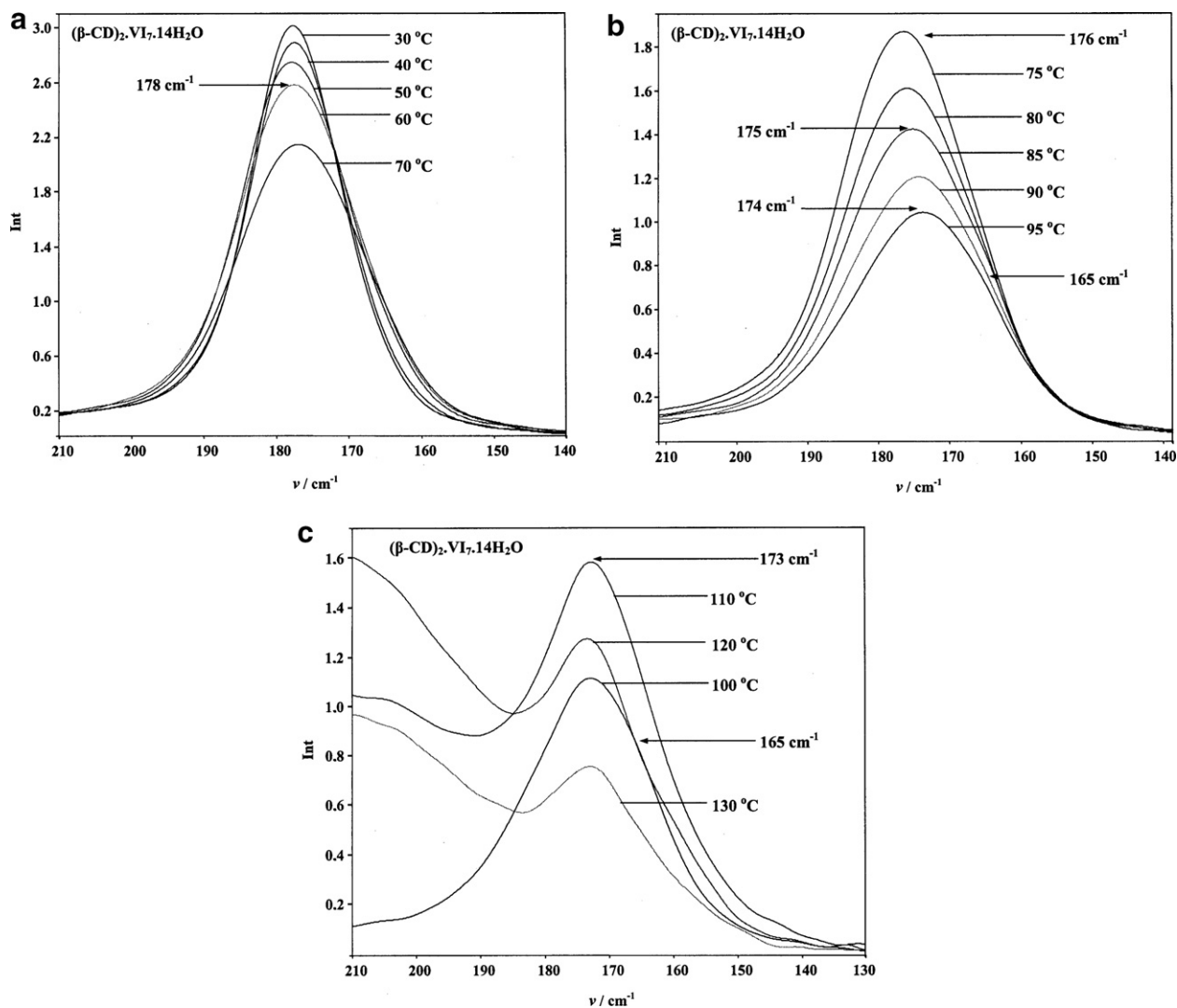
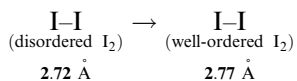


Figure 8. Raman spectra of $(\beta\text{-CD})_2\cdot\text{VI}_7\cdot 14\text{H}_2\text{O}$ during heating, in the temperature ranges of (a) 30–70 °C, (b) 75–95 °C and (c) 100–130 °C.



This progressive transformation involves many intermediate states of I–I lengthening that are directly related to the intermediate Raman bands that appear during the shift of $178 \rightarrow 166 \text{ cm}^{-1}$. Thus, it becomes clear that the relative populations of the two coexistent kinds of iodine molecules change inversely (the disordered I_2 units decrease, whereas well-ordered ones increase) as a function of temperature. This procedure is depicted in Figures 4b and 5a and b where the intermediate bands become more intense in comparison to the band at 178 cm^{-1} . Furthermore, the observed isosbestic point at 170 cm^{-1} in Figure 4b confirms the existence of two distinct kinds of iodine molecules whose spectra overlap. At $140 \text{ }^\circ\text{C}$, the band at 166 cm^{-1} is shifted to 173 cm^{-1} due to the sublimation of iodine which shortens the I_7^- units providing conduction paths along the polyo-

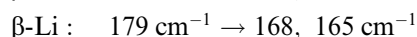
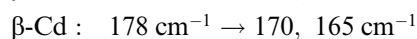
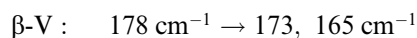
vide chains.^{2–4,12} As this process is in progress, the $\text{I}_2 \cdot \cdot \text{I}_3^-$ interactions become attenuated, resulting in a shortening of the I_2 bond lengths that is responsible for the shift of the ν_1 mode to higher wavenumbers. All of the above Raman spectral data reveal that the heptaiodide ions of $\beta\text{-Na}$ and $\beta\text{-Rb}$ display the same geometric shape with those of $\beta\text{-Ba}$, $\beta\text{-K}$ and $\beta\text{-Cs}$, indicating symmetric interactions of the central I_3^- with the two I_2 units.

The Raman spectra of $\beta\text{-Sr}$ and $\beta\text{-Bi}$ exhibit a gradual shift (intermediate bands appear) of the initial band at 178 cm^{-1} to a final single band, suggesting a symmetric charge-transfer interaction $\text{I}_2 \leftarrow \text{I}_3^- \rightarrow \text{I}_2$ as in the case of $\beta\text{-Na}$ and $\beta\text{-Rb}$. However, the final single bands of $\beta\text{-Sr}$ and $\beta\text{-Bi}$ are located at the frequencies of 170 cm^{-1} and 172 cm^{-1} , respectively, which are higher than the value of 166 cm^{-1} that was found for $\beta\text{-Na}$ and $\beta\text{-Rb}$. Considering the aforementioned correlation $\nu(\text{I-I}) - d(\text{I-I})$ ^{10,11}, the frequency of 170 cm^{-1} in the spectrum

of β -Sr corresponds to an I–I distance of 2.75 Å that is shorter than 2.77 Å (165–166 cm^{-1}). Regarding β -Bi, the frequency of 172 cm^{-1} shows that the final intramolecular distance of the iodine molecules is even shorter than the value of 2.75 Å (β -Sr). These experimental results indicate that the electron density donation of I_3^- to the attached I_2 units is stronger in β -Sr than in β -Bi. Nevertheless, both systems present a weaker charge-transfer interaction than that of β -Na and β -Rb complexes.

4.2. Non-symmetric $\text{I}_2 \cdots \text{I}_3^-$ interactions

In the Raman spectra of β -V, the initial band at 178 cm^{-1} is not shifted to a single band but to a double one of frequencies 173 and 165 cm^{-1} , indicating a disorder–order transition of the I_2 molecules via an unequal charge-transfer interaction ($\text{I}_2 \leftarrow \text{I}_3^- \rightarrow \text{I}_2$). This spectral behaviour is similar to that of β -Li and β -Cd^{2,4} according to the scheme:



The fact that at 30 °C the β -Li, β -Cd and β -V complexes exhibit a single band at the same frequency (178–179 cm^{-1}) implies a similar mean I–I distance (~ 2.72 Å) of the disordered iodine molecules in the β -CD cavities. However, the existence of double bands at elevated temperatures suggests that in each hepta-iodide ($\text{I}_2 \cdot \text{I}_3^- \cdot \text{I}_2$) the triiodide donor presents non-symmetric interactions with the two attached iodine molecules. The higher frequency (173, 170 and 168 cm^{-1}) of these double bands corresponds to the I_2 unit that interacts weakly with the central I_3^- , whereas the lower frequency of 165 cm^{-1} , which is common for the three complexes, corresponds to the other I_2 unit that interacts more strongly with I_3^- . The final intramolecular distance of the former I_2 unit decreases in the order β -Li, β -Cd and β -V and is shorter than 2.77 Å in contrast to the latter I_2 unit whose final intramolecular distance is equal to 2.77 Å.

4.3. The influence of metal's ionic potential

The ability of I_3^- to act as a Lewis base donor depends on the relative position of the different metal ions and their ionic potential q/r , where q is the charge and r the ionic radius.¹³ The greater the ionic potential is, the more the cation will interact with the triiodide ion. Table 1 shows a correlation between the increasing ionic potential of all the above metal ions and the observed band shift in the Raman spectra of the corresponding β -CD polyiodide complexes. It becomes apparent that in the case of Cs^+ , Rb^+ , K^+ , Na^+ and Ba^{2+} ions, the

Table 1. Correlation between the ionic potential (q/r) of the reported metals and the band shift in the Raman spectra of the corresponding β -CD polyiodide complexes

Metal ion	Ionic radius (Å)	Ionic potential (q/r)	Shift of the Raman band (cm^{-1})
Cs^+	1.69	0.59	179→166
Rb^+	1.48	0.67	178→166
K^+	1.33	0.75	179→165
Na^+	0.95	1.05	178→166
Ba^{2+}	1.35	1.48	179→166
Li^+	0.60	1.66	179→168, 165
Sr^{2+}	1.13	1.77	178→170
Cd^{2+}	0.97	2.06	178→170, 165
Bi^{3+}	0.92	3.26	178→172
V^{3+}	0.74	4.05	178→173, 165

final Raman frequency has the common value of 165–166 cm^{-1} even though their ionic potential ranges from 0.59 to 1.48. This means that there is not any specific interaction between these metals and the I_3^- ions (negligible $\text{M}^{n+} \cdots \text{I}_3^-$ interactions) (Fig. 9a). On the contrary, the two final frequencies of β -Li (168, 165 cm^{-1}), β -Cd (170, 165 cm^{-1}) and β -V (173, 165 cm^{-1}) and the final single frequencies of β -Sr (170 cm^{-1}) and β -Bi (172 cm^{-1}) reveal important $\text{M}^{n+} \cdots \text{I}_3^-$ interactions. This is due to the fact that the ionic potential of Li^+ , Sr^{2+} , Cd^{2+} , Bi^{3+} and V^{3+} ions ranges from 1.66 to 4.05. It is noteworthy, that metal–triiodide interactions are only observed when the ionic potential is greater than the critical value of ~ 1.50 .

Concerning β -Sr and β -Bi, the final single bands at 170 and 172 cm^{-1} , respectively, reveal face-on positions for Sr^{2+} and Bi^{3+} ions relative to the I_3^- ion (Fig. 9b). Thereby, each one of these cations presents equal interactions with the partial negative charge of the terminal I atoms (I(1), I(3)) of I_3^- ,^{14,15} attenuating their electron-donor ability. But since the ionic potential of Bi^{3+} (3.26) is greater than that of Sr^{2+} (1.77) the attenuation of the symmetric charge-transfer interaction $\text{I}_2 \leftarrow \text{I}_3^- \rightarrow \text{I}_2$, is more effective in β -Bi than in β -Sr. Therefore, in β -Sr the final bond distance of the I_2 units is 2.75 Å, whereas in β -Bi the corresponding bond distance is shorter than 2.75 Å. In the case of β -Li, β -Cd and β -V complexes, the situation is more complicated. The two coexistent bands at high-temperatures are pointing towards a side-on position of Li^+ , Cd^{2+} and V^{3+} ions relative to the I_3^- unit as it is shown in Figure 9c. This geometry results in a distorted I_3^- ion whose I–I bond (r_2) nearest to the cation is longer than the other one (r_1) and its terminal I atom (I(3)) nearest to the cation presents a greater negative charge (better e^- donor) than the other terminal I (I(1)).^{14,16} Thus, there is not an equal distribution of electronic density on the terminal I atoms, as in the case of a symmetric I_3^- ,^{14,17,18} and this indicates unequal charge-transfer interactions with the two I_2 units of each hepta-iodide ($\text{I}_2 \leftarrow \text{I}_3^- \rightarrow \text{I}_2$). More specifically, the disordered I_2 molecule that is attached

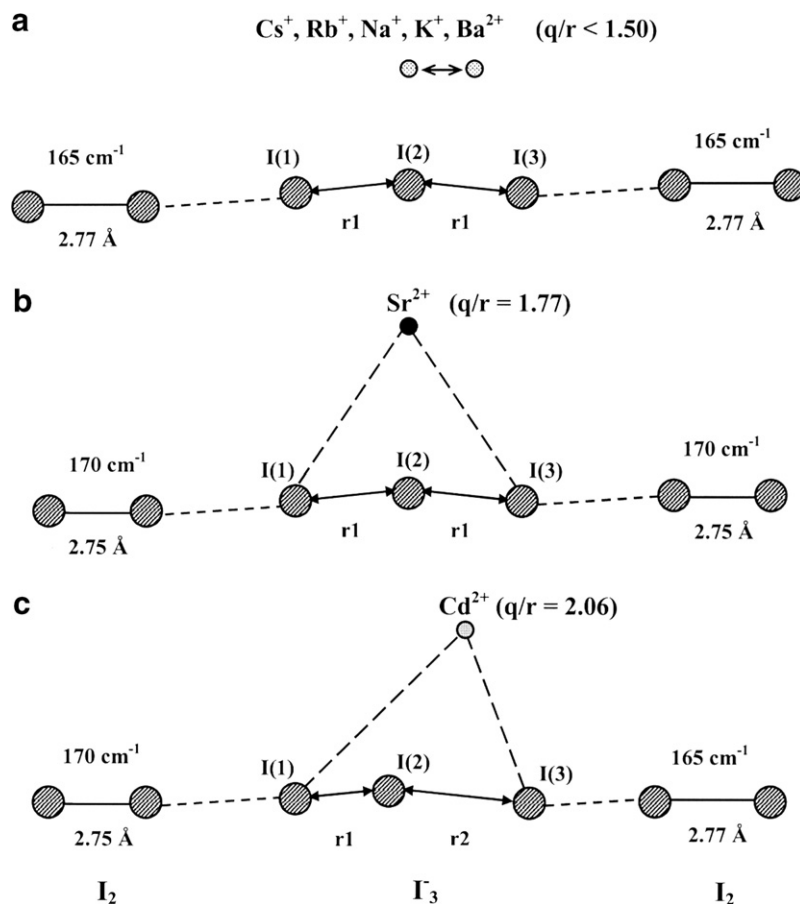


Figure 9. Schematic representation of the cation–triiodide interactions in the β -CD polyiodide complexes. The I_2 units of I_7^- have become well-ordered (disorder–order transition) and the hepta-iodide structure is viewed along the a -axis: (a) The position of Cs^+ , Rb^+ , Na^+ , K^+ and Ba^{2+} ions ($q/r < 1.50$) relative to the I_3^- ion does not exert any specific influence on the e^- donor ability of the terminal $\text{I}(1)$ and $\text{I}(3)$ atoms. (b) The Sr^{2+} ion ($q/r = 1.77$) presents a face-on position relative to I_3^- and interacts equally with the two terminal atoms $\text{I}(1)$ and $\text{I}(3)$ (similarly for Bi^{3+}). (c) The Cd^{2+} ($q/r = 2.06$) presents a side-on position relative to I_3^- and interacts asymmetrically with the two terminal atoms $\text{I}(1)$ and $\text{I}(3)$ (similarly for Li^+ and V^{3+}).

to the triiodide's $\text{I}(3)$ atom will become more elongated (lower wavenumber) than the other I_2 during the disorder–order transition.⁶ An interesting observation is that as the ionic potential increases in the following order Li^+ , Cd^{2+} , V^{3+} , the Lewis base character of the $\text{I}(1)$ atom becomes even more limited, whereas the Lewis base character of the $\text{I}(3)$ atom remains essentially unaffected.

Finally, it has been shown that the symmetric I_3^- ion with an I–I distance of 2.90 \AA has a Raman ν_1 mode at approximately 110 cm^{-1} .¹⁹ In our case, the intraiodine distance of I_3^- units is longer than 2.90 \AA ,¹ and the corresponding ν_1 mode is located at frequencies near or below 100 cm^{-1} . Thus, this band could not be detected due to the limited frequency range of the spectrometer ($\geq 100 \text{ cm}^{-1}$). When the I_3^- ions present distortions (lowering of symmetry), the other two modes ν_2 (50 – 70 cm^{-1}) and ν_3 (125 – 150 cm^{-1}) are expected to become Raman active.^{15,16,20,21} However, the ν_3 band was not observed in the Raman spectra of β -Li, β -Cd^{2,4} and β -V. This fact points to a weak distortion of the I_3^- ion,

which implies a small difference between the $r1$ and $r2$ bond lengths ($\Delta d = r2 - r1 \leq 0.1 \text{ \AA}$).¹⁵ Under this point of view, the $\text{M}^{n+} \cdots \text{I}(3)$ interactions seem to be slightly stronger than the $\text{M}^{n+} \cdots \text{I}(1)$ ones, justifying the e^- donor ability of the outer $\text{I}(1)$ atom. In the case of a large distortion, the $\text{I}(1)$ atom would not be able to donate electron density.¹⁴ We do not proceed to any further interpretation since the only method that can define the accurate I–I bond lengths is the detailed crystallographic study by an expert. Nevertheless, the observation of the band shift in the Raman spectra appears to be sufficient for the sake of this research, revealing that the metals exert a specific influence on the hepta-iodide interactions above a critical value (~ 1.50) of the ionic potential.

5. Conclusions

Raman spectroscopy provides sufficient information about the hepta-iodide structural changes of the β -CD

polyiodide inclusion complexes with Na^+ , Rb^+ , Sr^{2+} , Bi^{3+} and V^{3+} ions, during the heating process in the range of 30–140 °C. More specifically:

- (i) All of the five inclusion complexes present an initial Raman band at the common frequency of 178 cm^{-1} . This indicates that in each system the disordered iodine molecules present a mean intramolecular distance of $\sim 2.72\text{ \AA}$.
- (ii) The $\beta\text{-Na}$ and $\beta\text{-Rb}$ complexes display the band shift $178\rightarrow 166\text{ cm}^{-1}$ that is assigned to a disorder–order transition of the I_2 units via a symmetric charge-transfer interaction $\text{I}_2\leftarrow\text{I}_3^-\rightarrow\text{I}_2$. This process implies an elongation of the intramolecular I–I distance from 2.72 \AA (disordered state) to 2.77 \AA (well-ordered state). This spectral behaviour is similar to that of the previously investigated $\beta\text{-Ba}$, $\beta\text{-K}$ and $\beta\text{-Cs}$ complexes.
- (iii) In the case of the $\beta\text{-Sr}$ and $\beta\text{-Bi}$ complexes, the corresponding band shifts are $178\rightarrow 170\text{ cm}^{-1}$ and $178\rightarrow 172\text{ cm}^{-1}$, respectively. These spectral data also reveal a symmetric charge-transfer interaction $\text{I}_2\leftarrow\text{I}_3^-\rightarrow\text{I}_2$ as in the case of the $\beta\text{-Na}$ and $\beta\text{-Rb}$ complexes. However, the final intramolecular distance of the I_2 units is 2.75 \AA for $\beta\text{-Sr}$ and shorter than 2.75 \AA for $\beta\text{-Bi}$. Therefore, both systems present weaker charge-transfer interactions than those of the $\beta\text{-Na}$ and $\beta\text{-Rb}$ complexes.
- (iv) Concerning $\beta\text{-V}$, the initial band at 178 cm^{-1} is shifted to a double band of frequencies 173 and 165 cm^{-1} , indicating a disorder–order transition of the I_2 molecules via a non-symmetric charge-transfer interaction ($\text{I}_2\leftarrow\text{I}_3^-\rightarrow\text{I}_2$). The higher frequency (173 cm^{-1}) of this double band corresponds to the I_2 unit that interacts weakly with the central I_3^- , whereas the lower frequency (165 cm^{-1}) corresponds to the other I_2 unit that interacts more strongly with I_3^- . This spectral behaviour is similar to that of the previously investigated $\beta\text{-Li}$ ($179\rightarrow 168$, 165 cm^{-1}) and $\beta\text{-Cd}$ ($178\rightarrow 170$, 165 cm^{-1}).
- (v) All the above results reveal that cations which present an ionic potential that is lower than ~ 1.50 (Cs^+ , Rb^+ , Na^+ , K^+ and Ba^{2+}) do not affect the Lewis base character of I_3^- . However, when the ionic potential of the cation is greater than ~ 1.50 (Li^+ , Sr^{2+} , Cd^{2+} , Bi^{3+} and V^{3+}), the Lewis base character of I_3^- is affected and depends on the relative position of M^{n+} . In the case of a face-on position (Sr^{2+} , Bi^{3+}), the charge-transfer

interaction is symmetric. On the contrary, when the metal (Li^+ , Cd^{2+} , V^{3+}) presents a side-on position relative to I_3^- , the charge-transfer interaction is non-symmetric.

Acknowledgements

This work was carried out in partial fulfilment of the requirements for V.G.C.'s PhD Thesis. It was partly supported by Grant No. 70/4/3347SARG, NKUA. We are grateful to Professor K. Viras for his assistance in conducting the Raman Spectra.

References

1. Betzel, C.; Hingerty, B.; Noltemeyer, M.; Weber, G.; Saenger, W.; Hamilton, J. A. *J. Inclusion Phenom. Macrocyclic Chem.* **1983**, *1*, 181–191.
2. Charalampopoulos, V. G.; Papaioannou, J. C. *Mol. Phys.* **2005**, *103*, 2621–2631.
3. Charalampopoulos, V. G.; Papaioannou, J. C.; Karayianni, H. S. *Solid State Sci.* **2006**, *8*, 97–103.
4. Papaioannou, J. C.; Charalampopoulos, V. G.; Xynogalas, P.; Viras, K. *J. Phys. Chem. Solids* **2006**, *67*, 1379–1386.
5. Moreira da Silva, A. M. G.; Steiner, T.; Saenger, W.; Empis, J. M. A.; Teixeira-Dias, J. J. C. *J. Inclusion Phenom. Mol. Recognit. Chem.* **1996**, *25*, 21–24.
6. Anderson, A.; Sun, T. S. *Chem. Phys. Lett.* **1970**, *6*, 611–616.
7. Papaioannou, J. C. *Mol. Phys.* **2004**, *102*, 95–99.
8. Papaioannou, J. C.; Papadimitropoulos, N.; Mavridis, I. *Mol. Phys.* **1999**, *97*, 611–627.
9. Steiner, T.; Koellner, G. *J. Am. Chem. Soc.* **1994**, *116*, 5122–5128.
10. Deplano, P.; Devillanova, F. A.; Ferraro, J. R.; Isaia, F.; Lippolis, V.; Mercuri, M. L. *Appl. Spectrosc.* **1992**, *46*, 1625–1629.
11. Demartin, F.; Deplano, P.; Devillanova, F. A.; Isaia, F.; Lippolis, V.; Verani, G. *Inorg. Chem.* **1993**, *32*, 3694–3699.
12. Oza, A. *Cryst. Res. Technol.* **1984**, *19*, 697–707.
13. Railsback, L. B. *Geology* **2003**, *31*, 737–740.
14. Novoa, J. J.; Mota, F.; Alvarez, S. *J. Phys. Chem.* **1988**, *92*, 6561–6566.
15. Svensson, P. H.; Kloo, L. *Chem. Rev.* **2003**, *103*, 1649–1684.
16. Svensson, P. H.; Kloo, L. *J. Chem. Soc., Dalton Trans.* **2000**, 2449–2455.
17. Landrum, G. A.; Goldberg, N.; Hoffmann, R. *J. Chem. Soc., Dalton Trans.* **1997**, 3605–3613.
18. Lin, Z.; Hall, M. B. *Polyhedron* **1993**, *12*, 1499–1504.
19. Nour, E. M.; Chen, L. H.; Laane, J. J. *J. Phys. Chem.* **1986**, *90*, 2841–2846.
20. Mittag, H.; Stegemann, H.; Füllbier, H.; Irmer, G. *J. Raman Spectrosc.* **1989**, *20*, 251–255.
21. Yu, X.; Atalla, R. H. *Carbohydr. Res.* **2005**, *340*, 981–988.